AIP | APL Materials

Evidence for spin to charge conversion in GeTe(111)

C. Rinaldi, J. C. Rojas-Sánchez, R. N. Wang, Y. Fu, S. Oyarzun, L. Vila, S. Bertoli, M. Asa, L. Baldrati, M. Cantoni, J.-M. George, R. Calarco, A. Fert, and R. Bertacco

Citation: APL Mater. **4**, 032501 (2016); doi: 10.1063/1.4941276
View online: http://dx.doi.org/10.1063/1.4941276
View Table of Contents: http://scitation.aip.org/content/aip/journal/aplmater/4/3?ver=pdfcov
Published by the AIP Publishing

Evidence for spin to charge conversion in GeTe(111)

C. Rinaldi,[1,2] J. C. Rojas-Sánchez,[3,4] R. N. Wang,[5] Y. Fu,[6] S. Oyarzun,[6] L. Vila,[6] S. Bertoli,[1] M. Asa,[1] L. Baldrati,[1] M. Cantoni,[1] J.-M. George,[3] R. Calarco,[5] A. Fert,[3] and R. Bertacco[1,2]
[1]*Dipartimento di Fisica, Politecnico di Milano, Via Colombo 81, 20133 Milano, Italy*
[2]*IFN-CNR, c/o Politecnico di Milano, Via Colombo 81, 20133 Milano, Italy*
[3]*Unité Mixte de Physique, CNRS, Thales, Univ. Paris-Sud, Université Paris-Saclay, 91767 Palaiseau, France*
[4]*Institut Jean Lamour, UMR CNRS-Université de Lorraine, 54506 Vandouevre lès Nancy, France*
[5]*Paul-Drude-Institut für Festkörperelektronik, Hausvogteiplatz 5-7, 10117 Berlin, Germany*
[6]*Université Grenoble Alpes and CEA, INAC–SP2M, F-38000 Grenoble, France*

(Received 4 December 2015; accepted 21 January 2016; published online 11 February 2016)

GeTe has been predicted to be the father compound of a new class of multifunctional materials, ferroelectric Rashba semiconductors, displaying a coupling between spin-dependent k-splitting and ferroelectricity. In this paper, we report on epitaxial Fe/GeTe(111) heterostructures grown by molecular beam epitaxy. Spin-pumping experiments have been performed in a radio-frequency cavity by pumping a spin current from the Fe layer into GeTe at the Fe ferromagnetic resonance and detecting the transverse charge current originated in the slab due to spin-to-charge conversion. Preliminary experiments indicate that a clear spin to charge conversion exists, thus unveiling the potential of GeTe for spin-orbitronics. [http://dx.doi.org/10.1063/1.4941276]

In the recent years, there has been a renewed interest in materials and heterostructures exploiting spin-orbit coupling as key ingredient to modulate transport and micromagnetic properties. Beyond classical spintronics,[1] the emerging field of spin-orbitronics aims to generate, manipulate, and detect pure spin currents in nonmagnetic materials.[2] In bulk materials, this is achieved via intrinsic or extrinsic Spin Hall effect (SHE) and inverse Spin Hall effect (ISHE), allowing for charge-to-spin and spin-to-charge current (SCC) conversions, respectively.[3,4] For Rashba states in 2DEG systems, as well as topological states at surfaces, the same conversion phenomena correspond to the direct and inverse Rashba-Edelstein Effect (REE).[5] So far, materials with high atomic numbers (e.g. Pt, Ta, Au, and Bi) have been mainly used in bulk form for SHE and to create interface states displaying REE. The search for new materials, compatible with semiconductor technology and displaying even stronger Rashba parameters, is crucial in order to improve the charge-to-spin conversion and bridge the gap towards applications.

Recently, a new class of multifunctional semiconductors with great potential for spin-orbitronics has been introduced: Ferroelectric Rashba SemiConductors (FERSCs).[6] They are predicted to display an intrinsic link between ferroelectric polarization and spin chirality in Rashba bands, thus paving the way to the electric control of spin transport properties through the manipulation of the ferroelectric polarization. Their father compound, GeTe, is a well known chalcogenide semiconductor, widely investigated in the framework of phase-change materials. Below 720 K, GeTe displays a non-centrosymmetric ferroelectric structure (space group R3m (No. 160)), with Ge and Te ions displaced from the ideal rocksalt sites along the [111] direction, so as to display a remanent ferroelectric polarization.[7–9] This breaks the inversion symmetry and gives rise to bulk Rashba-type bands, especially along the ZA and ZU directions lying in the hexagonal face of the first Brillouin zone and parallel to the [−110] and [11-2] directions in the direct space, when adopting a pseudo-cubic notation for GeTe. Record values of the Rashba parameters have been predicted (k_R = 0.09 Å^{-1}, E_R = 227 meV, α_R = 5 eV · Å along ZA), even with respect to the polar semiconductor BiTeI.[10]

Recently, some of us experimentally established, via Piezo-Force Microscopy (PFM) and spin and angular resolved photoemission spectroscopy (ARPES), the relation between Rashba bands spin helicity and non-volatile ferroelectric polarization in GeTe(111) films.[11] Furthermore, novel surface Rashba states have been identified, with record Rashba wave vector splitting $k_R = 0.14$ Å^{-1}, much larger than in any conventional semiconductor and metal surface.[12,13]

In this paper, we provide the first experimental evidence for a spin-to-charge current conversion in GeTe via spin pumping-ferromagnetic resonance experiments on Fe/GeTe(111) epitaxial bilayers. α-GeTe(111) 75 nm thick films have been grown by Molecular Beam Epitaxy (MBE)[14] on Si(111) substrates (p-type B-doped, 1-10 Ωcm resistivity, and ±0.038° miscut) starting from a Si(111) with a $(\sqrt{3} \times \sqrt{3})$R30°-Sb reconstruction which suppresses the formation of rotational domains.[15] After growth, GeTe films have been capped with Si_3N_4 *in situ* and then transferred to another MBE machine[16] for metals and oxides. The recipe for re-preparing a good GeTe(111) surface consists in: (i) wet etching in buffered hydrofluoric acid to remove the Si_3N_4 capping layer and (ii) annealing in UHV to remove contaminants and order the surface. The morphology after Si_3N_4 removal is shown in Figure 1(a), where an atomic force microscopy image is reported over a 10×10 μm^2 area. The film is made of triangular terraces, merging together in most of the sample surface but leaving some holes with depth comparable with the film thickness. Within each terrace, the film is atomically flat, with 0.4 nm rms roughness, while the average roughness is about 4 nm. The topography nicely resembles that of as-grown samples.[15]

A systematic study of the impact of the annealing temperature, between 200 and 350 °C, on the surface order and stoichiometry has been carried out by Low Energy Electron Diffraction (LEED) and X-ray Photoemission Spectroscopy (XPS). The typical line shape of *Te* 4*d* and *Ge* 3*d* core

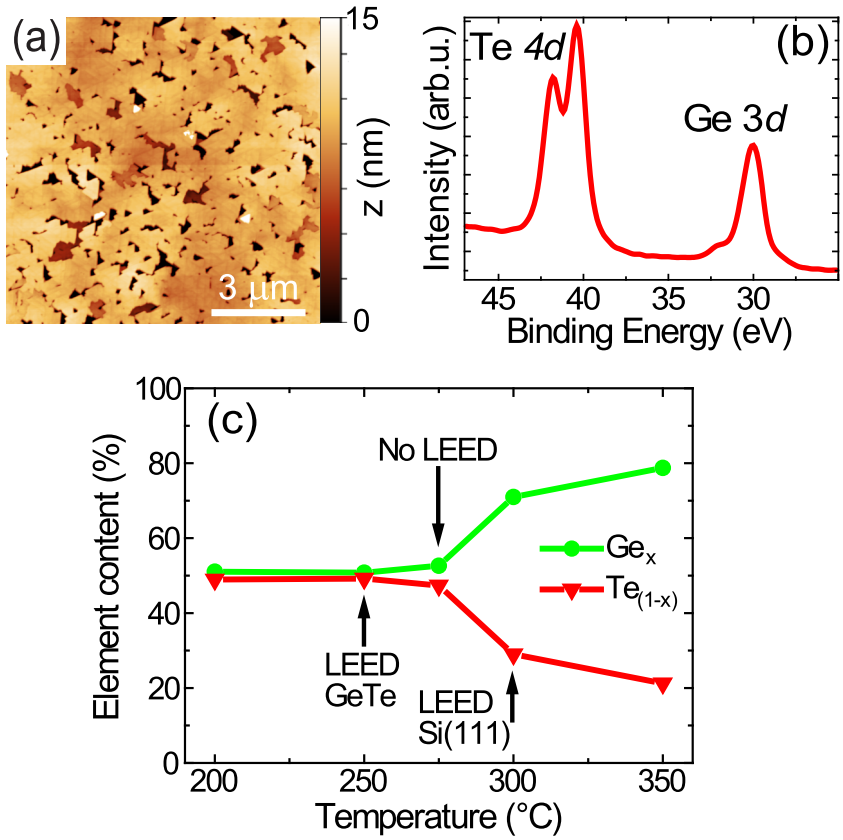

FIG. 1. (a) Atomic force microscopy image of the GeTe(111) surface after Si_3N_4 stripping. (b) XPS spectrum taken with Al-Kα radiation after annealing in vacuum at 250 °C. (c) Evolution of the surface stoichiometry as a function of the annealing temperature.

levels after annealing is reported in Figure 1(b), showing a clean surface with only a minor Ge oxidation indicated by the shoulder at about 32 eV binding energy in the *Ge* 4*d* spectrum. The evolution of the surface chemical composition from *Te* 4*d* and *Ge* 3*d* intensities is reported in Figure 1(c), for annealing at incremental temperatures with steps of 20 min at each of them. 250 °C are required for the six-fold LEED of GeTe to show up, while at 275 °C, the LEED pattern disappears and the stoichiometry becomes Ge-rich due to the preferential Te evaporation. Above 300 °C, GeTe almost completely evaporates and the typical LEED pattern from the Si(111) substrate is recovered. Based on this analysis, samples for spin pumping have been annealed at 250 °C, so as to obtain a well ordered surface with nominal stoichiometry: $Ge_{0.50\pm0.03}Te_{0.50\pm0.03}$. The corresponding LEED pattern is shown in Figure 2(a). On this ordered surface, a 5 nm thick Fe film has been grown by MBE at room temperature. Due to the relatively small mismatch between the Fe(111) and GeTe(111) planes (2.9% assuming a lattice constant of 2.8665 Å for bcc Fe and an in-plane lattice parameter of 4.174 Å for GeTe[15]), Fe is supposed to epitaxially grow in register on GeTe(111). Indeed, the LEED pattern of Figure 2(b) shows the hexagonal symmetry of the surface, corroborating such assumption.

The magnetic properties of the film have been investigated by vibrating sample magnetometry. Figure 2(c) reports an hysteresis loop taken by sweeping the magnetic field along the GeTe[-110] direction. A polar plot of the coercive field as a function of the angle ϕ between the applied magnetic field and GeTe[-110] direction (corresponding to the ZA direction in the reciprocal space) is shown in Figure 2(d). A minor trace of four-fold magnetic anisotropy is seen, with the coercive field varying between 19 Oe and 24 Oe. This is in agreement with the Fe/Si(111) system[17] and can be attributed to the competition between cubic magnetic anisotropy, out of plane demagnetizing field, and anisotropy contributions coming from the substrate miscut.

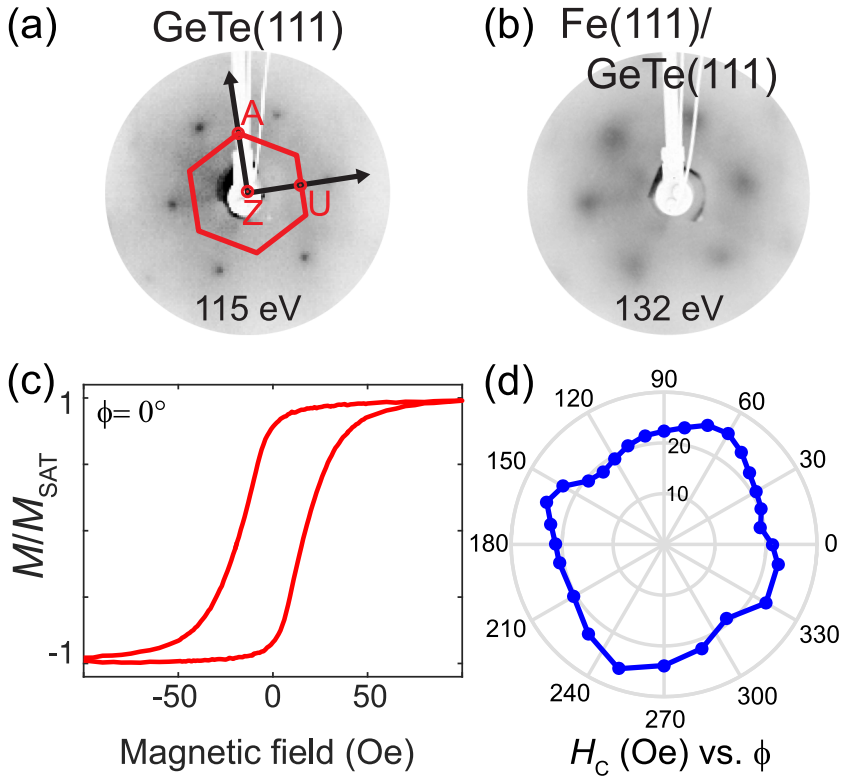

FIG. 2. (a) LEED pattern from the re-prepared GeTe(111) surface taken at 115 eV with the hexagonal face of the first Brillouin zone centered at Z. (b) LEED from a 5 nm thick Fe film epitaxially grown on the surface of panel (a). (c) Hysteresis loop of the magnetization (M) normalized to the saturation magnetization (M_{SAT}) for an applied magnetic field at an angle $\phi = 0$ with respect to the GeTe[-110] (ZA) direction. (d) Polar plot of the coercive field (H_c) from in-plane hysteresis loops as a function of ϕ.

We have checked the ferroelectric behaviour of GeTe films upon surface re-preparation by PFM. PFM point spectroscopy loops (data not shown) are very similar to that reported in Ref. 11, thus providing evidence for a uniform virgin state polarization. This arises from the thermodynamic stability of the Te-terminated surface of α-GeTe(111),[18] which promotes this termination during growth or preparation.[15] As a result of the shorter Ge-Te bonds' arrangement at the very surface, the intrinsic dielectric surface dipole points outwards. This provides the symmetry-breaking necessary to establish Rashba bands with well defined helicity over the macroscopic sample area used for spin-pumping, without the need of sample poling.

Spin Pumping-Ferromagnetic Resonance (SP-FMR) experiments[4,19–21] have been performed to probe the SCC conversion. An epitaxial Si(111)/GeTe(75)/Fe(5) stack (thicknesses in nm) was grown as described above and capped with 3 nm of Au to prevent Fe oxidation. We studied rectangular slabs cut along the two high-symmetry ZA and ZU directions of GeTe in the ZAU plane where Rashba splitting is maximum. The slabs were placed at the center of a cylindrical cavity, and their FMR response compared to that of a Si(111)/Fe(5)/Au(5) reference sample. At the resonance condition, the adjacent GeTe layer opens a relaxation channel to the precessing magnetization and a transfer of angular momentum from the Fe layer occurs. This is seen in the extra damping enhancement while studying the FMR at variable frequencies (data not shown). Due to spin-orbit coupling, the spin current injected from the Fe layer is converted into a transverse charge current. As GeTe displays both bulk and surface Rashba bands,[11] either ISHE or inverse Edelstein effect (IEE) can be involved. As a result, when conversion from spin-to-charge current occurs, a transverse dc voltage appears when using the electrical probe configuration schematized in Figure 3(a). Preliminary room temperature measurements along the ZA direction of GeTe are shown in Figures 3(b) and 3(c), where a dc transverse voltage is observed at the Fe resonance field. The following features are in agreement with a SCC origin of the phenomenon: (i) the voltage has a clear symmetric Lorentzian shape, (ii) the linewidth ($\mu_0 H_{pp}$ = 10 mT) is enlarged with respect to the reference sample ($\mu_0 H_{pp}$ = 5.5 mT, data not shown), consistently with an additional spin absorption

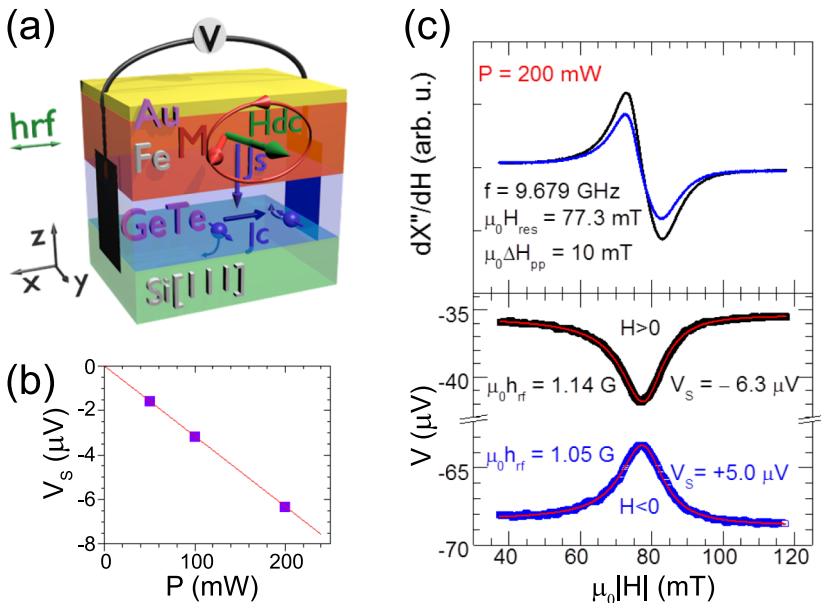

FIG. 3. (a) Scheme of the Si//GeTe(75 nm)/Fe(5 nm)/Au(3 nm) slab under ferromagnetic resonance condition. The RF field (h_{RF}) is applied along the ZA direction (x axis), while the dc field (H_{dc}) around which the magnetization precesses is along the y axis. A spin current J_s is injected from the Fe layer into GeTe, which in turn converts this spin current into a charge current J_c, detected by measuring the transverse voltage V in open circuit configuration. (b) Raw data of simultaneous measurements of FMR spectrum (top panel) and transverse voltage V (bottom panel). Black (blue) curves correspond to positive (negative) *y* components of H_{dc}, while red lines are Lorentzian fittings. (c) Power dependence of the voltage amplitude. The measurements were performed at room temperature.

by GeTe, and (iii) the voltage is reversed when the external dc magnetic field is reversed. Additionally, in Figure 3(c), the power dependence of the transversal voltage amplitude is shown. This further evidences the linear regime of SP-FMR and allows disregarding thermal effects which are expected to be highly non-linear.[22] In contrast to Figure 3(b), the Si(111)/Fe/Au reference sample shows mostly antisymmetric transversal voltage and has a smaller linewidth than the GeTe sample (data not shown). Note that the value of the linewidth in the reference sample (5.5 mT at 9.6 GHz) is larger than that expected for Fe (about 2 mT), probably due to the roughness of the Fe film mimicking that of GeTe (see Figure 1(a)). No voltage was instead detected in slabs cut along the ZU direction. This gets rid of the possibility that the observed signal is coming from the Au layer, for which we have measured a spin Hall angle of 0.0044 and a spin diffusion length much larger than 3 nm.[23]

At this stage, we cannot compute a reliable value of the spin mixing conductivity and thus injected spin current due to the anomalous behavior of the FMR linewidth in the reference sample. Besides, it is not possible to know if the SCC has its origin from bulk, interface, or both. The voltage amplitude, normalized by the sample resistance and square of the radiofrequency (RF) field, h_{rf}, leads to a charge current production of $I_c/h_{rf}^2 = -29$ nA/G^2. This is a rather small value in comparison with spin pumping experiments performed by using similar sizes of similar magnetic materials (FeNi or Fe) on Pt (500 nA/G^2),[4] Ag/Bi Rashba interface (about 600 nA/G^2),[5] or α-Sn thin films topological insulator (2 μA/G^2).[24] However, it has been recently pointed out by ARPES that the direct contact of the FM layer might be detrimental in the case of IEE.[24] This could explain the low current production. Another interesting feature is that the charge current production of GeTe is opposite to that found in Pt.

Further studies are required in order to quantify the SCC and to reveal if its origin is from bulk or interface. The insertion of spacer layers with long diffusion length and low spin-orbit coupling between Fe and GeTe is a suitable option to this scope. Furthermore, the connection between the absence of signal along ZU and the structure of Rashba bands must be carefully investigated. The switching of the voltage sign upon reversal of the ferroelectric polarization is the next step in view of the deployment of the intriguing peculiarities of GeTe, but this is beyond the scope of this paper. Here, we have demonstrated for the first time that spin-to-charge conversion is possible in GeTe. This is a fundamental milestone in the investigation of the potential of FERSC materials for spin-orbitronics, with the aim of bridging the gap between material properties and their deployment in spintronic devices.

The authors thank M. Leone, L. Livietti, and C. Somaschini, from Polifab–Politecnico di Milano, for technical assistance. This work was funded by Fondazione Cariplo via the project MAGISTER (Grant No. 2013-0726). R.W. and R.C. thank S. Behnke and C. Stemmler for technical support at the MBE system as well as partial support by EU within the FP7 Project PASTRY (GA No. 317746).

[1] S. Maekawa, *Concepts in Spin Electronics* (Oxford University Press, 2006).
[2] A. Manchon, Nat. Phys. **10**, 340 (2014).
[3] J. E. Hirsch, Phys. Rev. Lett. **83**, 1834 (1999).
[4] J. C. Rojas-Sánchez *et al.*, Phys. Rev. Lett. **112**, 106602 (2014).
[5] J. C. Rojas-Sánchez, L. Vila, G. Desfonds, S. Gambarelli, J. M. Attané, M. De Teresa, C. Magén, and A. Fert, Nat. Commun. **4**, 2944 (2013).
[6] D. Di Sante, P. Barone, R. Bertacco, and S. Picozzi, Adv. Mater. **25**, 509 (2013).
[7] J. Chattopadhyay, T. Boucherle, and H. Von Schnering, J. Phys. C: Solid State Phys. **20**, 1431 (1987).
[8] K. M. Rabe and J. D. Joannopoulos, Phys. Rev. B **36**, 6631 (1987).
[9] R. Shaltaf, E. Durgun, J.-Y. Raty, P. Ghosez, and X. Gonze, Phys. Rev. B **78**, 205203 (2008).
[10] K. Ishizaka, M. S. Bahramy, H. Murakawa, M. Sakano, T. Shimojima, T. Sonobe, K. Koizumi, S. Shin, H. Miyahara, A. Kimura, K. Miyamoto, T. Okuda, H. Namatame, M. Taniguchi, R. Arita, N. Nagaosa, K. Kobayashi, Y. Murakami, R. Kumai, Y. Kaneko, Y. Onose, and Y. Tokura, Nat. Mater. **10**, 521 (2011).
[11] M. Liebmann, C. Rinaldi, D. Di Sante, J. Kellner, C. Pauly, R. N. Wang, J. E. Boschker, A. Giussani, S. Bertoli, M. Cantoni, L. Baldrati, M. Asa, I. Vobornik, G. Panaccione, D. Marchenko, J. Sánchez-Barriga, O. Rader, R. Calarco, S. Picozzi, R. Bertacco, and M. Morgenstern, Adv. Mater. **28**, 560 (2015).
[12] A. M. Gilbertson, W. R. Branford, M. Fearn, L. Buckle, P. D. Buckle, T. Ashley, and L. F. Cohen, Phys. Rev. B **79**, 235333 (2009).
[13] Y. M. Koroteev, G. Bihlmayer, J. E. Gayone, E. V. Chulkov, S. Blügel, P. M. Echenique, and P. Hoffmann, Phys. Rev. Lett. **93**, 046403 (2004).

[14] A. Giussani, K. Perumal, M. Hanke, P. Rodenbach, H. Riechert, and R. Calarco, Phys. Status Solidi B **249**, 1939 (2012).
[15] R. Wang, J. E. Boschker, E. Bruyer, D. Di Sante, S. Picozzi, K. Perumal, A. Giussani, H. Riechert, and R. Calarco, J. Phys. Chem. C **118**, 29724 (2014).
[16] R. Bertacco *et al.*, Appl. Surf. Sci. **252**, 1754 (2005).
[17] H. F. Du *et al.*, Appl. Phys. Lett. **96**, 142511 (2010).
[18] V. L. Deringer, M. Lumeij, and R. Dronskowski, J. Phys. Chem. C **116**, 15801 (2012).
[19] K. Ando *et al.*, J. Appl. Phys. **109**, 103913 (2011).
[20] O. Mosendz, V. Vlaminck, J. E. Pearson, F. Y. Fradin, G. E. W. Bauer, S. D. Bader, and A. Hoffmann, Phys. Rev. B **82**, 214403 (2010).
[21] J. C. Rojas-Sánchez *et al.*, Phys. Rev. B **88**, 064403 (2013).
[22] Y. Shiomi *et al.*, Phys. Rev. Lett. **113**, 196601 (2014).
[23] P. Laczkowski *et al.*, Appl. Phys. Lett. **104**, 142403 (2014).
[24] J. C. Rojas-Sánchez *et al.*, preprint, arXiv:1509.02973 (2015).